Article

Normal Values for the Full Visual Field, Corrected for Age- and Reaction Time, Using Semiautomated Kinetic Testing on the Octopus 900 Perimeter

Julia Grobbel[1], Janko Dietzsch[1], Chris A. Johnson[4 ✉], Reinhard Vonthein[2], Katarina Stingl[1], Richard G. Weleber[3], and Ulrich Schiefer[1,5]

[1] Centre for Ophthalmology/Institute for Ophthalmic Research, University of Tübingen, Germany
[2] Institute for Medical Biometry and Statistics and the Center for Clinical Trials, University of Lübeck, Germany
[3] Casey Eye Institute, Oregon Health & Science University, Portland, OR, USA
[4] Department of Ophthalmology and Visual Sciences and Wynn Institute for Vision Research, University of Iowa, Iowa City, IA, USA
[5] Competence Center Vision Research, Study Course "Ophthalmic Optics and Audiology", Faculty of Optics and Mechatronics, University of Applied Sciences, Aalen, Germany

Correspondence: Chris A. Johnson, PhD, Department of Ophthalmology and Visual Sciences and Wynn Institute for Vision Research, University of Iowa Hospitals and Clinics, 200 Hawkins Drive, Iowa City, IA, USA 52242-1091; e-mail: chris-a-johnson@uiowa.edu

Purpose: To determine normal values of the visual field (VF), corrected for age and reaction time (RT) for semiautomated kinetic perimetry (SKP) on the Octopus 900 perimeter, create a model describing the age-dependency of these values, and assess test–retest reliability for each isopter.

Methods: Eighty-six eyes of 86 ophthalmologically healthy subjects (age 11–79 years, 34 males, 52 females) underwent full-field kinetic perimetry with the Octopus 900 instrument. Stimulus size, luminance, velocity, meridional angle, subject age, and their interactions, were used to create a smooth multiple regression mathematical model (V/4e, III/4e, I/4e, I/3e, I/2e, I/1e, and I/1a isopters). Fourteen subjects (2 from each of 7 age groups) were evaluated on three separate sessions to assess test–retest reliability of the isopters. Reaction time (RT) was tested by presenting 12 designated RT-vectors between 10° and 20° within the seeing areas for the III/4e isopter (stimulus velocity, 3°/second). Four RT- vectors were presented at the nasal (0° or 180°), superotemporal (45°), and inferior (270°) meridians.

Results: The model fit was excellent ($r^2 = 0.94$). The test–retest variability was less than 5°, and the median decrease in this deviation attributed to aging, per decade, for all age groups and for all stimulus sizes was 0.8°. No significant learning effect was observed for any age group or isopter.

Conclusion: Age-corrected and RT-corrected normative threshold values for full-field kinetic perimetry can be adequately described by a smooth multiple linear regression mathematical model.

Translational Relevance: A description of the entire kinetic VF is useful for assessing a full characterization of VF sensitivity, determining function losses associated with ocular and neurologic diseases, and for providing a more comprehensive analysis of structure–function relationships.

Introduction

Kinetic perimetry is the method of choice in cases of advanced visual field (VF) deficits,[1,2] as well as detecting early stages of VF loss. Compared with conventional automated static perimetry, kinetic testing is more sensitive for detecting peripheral VF defects,[3] less tedious and time-consuming (e.g., for subjects with pigmentary retinopathy),[4] more efficient for detection and monitoring progression of steep-edged field defects, has a greater flexibility for dynamic evaluation of the VF, provides more interaction between the examiner and the patient during testing, and the kinetic examination results correlate better with activities of daily living.[5,6] In

some countries, kinetic perimetry is used for qualification for a driver's license, assessment of disability, qualification for special support programs for the visually impaired, in the neuro-ophthalmologic evaluation of VF defects (e.g., hemianopsia, quadrantanopsia, concentric constriction), and assessment of retinal diseases affecting the peripheral VF. Kinetic perimetry is preferred over static perimetry for subjects with poor compliance, for evaluation of children, and for the detection of small, multiple VF defects in the periphery, which may be of meaningful clinical relevance.[7]

Using manual kinetic perimetry, a high quality assessment of the VF of a patient can be obtained in a short test time by a well-trained, knowledgeable, and experienced perimetrist. This is particularly true for the far peripheral VF. However, the acquisition of these skills and experience in manual kinetic perimetry requires considerable time and experience, up to 1 to 2 years of daily performance. In the Optic Neuritis Treatment Trial where kinetic peripheral testing on the Goldmann perimeter was employed, quality control scores were poorer for kinetic perimetry than for automated static perimetry of the central VF, in spite of a documented protocol, technician training and certification, and immediate feedback on testing procedures.[8] This illustrates the difficulties that can be encountered when all aspects of kinetic testing cannot be completely standardized for manual evaluations, even when careful and thorough protocols are employed and feedback is provided. In this view, better results with a shorter learning time may be expected using semiautomated kinetic perimetry (SKP), with the Octopus 900 perimeter (Haag Streit AG, Koeniz, Switzerland). SKP allows computer-controlled standardized presentation for any chosen Goldmann stimulus size-intensity combination, in any direction over the entire VF, with predefined starting and ending points for the stimulus vectors and constant angular velocities. Through computer control of stimulus presentation, SKP enables certain variables that affect performance of the examination to be made less dependent on the skills and experience of the perimetrist, thereby improving consistency and standardization of testing. Another benefit of kinetic testing using SKP is the ability to assess the reaction time (RT) for the subject for each VF session and subsequently to correct the position of the response on the basis of the individual RT of the subject. The advent of automated static perimetry has resulted in greater consistency, reliability, standardization, analysis and interpretation of VF results, but attempts to achieve automated kinetic perimetry have only recently been achieved.

Each kinetic VF should include at least three or four isopters drawn from the list of stimulus parameter sizes, luminance levels, and angular velocities that best define the full extent of the VF.[1] An understanding of the averages, standard deviations (SD), and ranges of age-adjusted normal values for the different stimulus parameters used for kinetic testing, and the test–retest variability of each of the stimulus parameter combinations is essential for distinguishing pathological VFs from normal variability. In this study, the VF was examined with seven different isopters and 24 stimulus presentations per isopter (except for the I/1e and I/1a isopters, which used 12 stimulus presentations per isopter due to space limitations) to fully characterize this relationship for SKP. To our knowledge, this study represents the first published report of normative values for of the entire VF for SKP using the Octopus 900 perimeter.

Automation of kinetic perimetry testing provides greater standardization of this VF procedure, similar to the improvements achieved with automated static perimetry. To provide further standardization of the testing and analysis of automated kinetic perimetry results, it was determined that a mathematical model should be produced from the results obtained from this investigation. The mathematical model created from our findings describes the age- and RT-corrected normative values for the entire VF, thus allowing the local threshold values of ophthalmologically healthy subjects to be quickly recognized from and compared to patients with VF defects.

Methods

Subjects

Following explanation of the study and the procedures that participants would undergo, written informed consent was obtained from all subjects. The study followed the tenets of the Declaration of Helsinki. In addition, written informed consent was obtained from the legal guardian for those under legal age. The study was approved by the ethics committee of the local institutional review board.

Detailed ophthalmological and general medical histories were recorded and a comprehensive ophthalmological examination on each participant was performed that included visual acuity, intraocular pressure (IOP), a color vision test (Ishihara and

Table 1. Stimulus Conditions Employed for This Investigation

Condition C	Stimulus Size	Stimulus Luminance	Angular Velocity
1	V/4e	320 cd/m2	5°/s
2	III/4e	320 cd/m2	5°/s
3	I/4e	320 cd/m2	5°/s
4	I/3e	100 cd/m2	5°/s
5	I/2e	32 cd/m2	3°/s
6	I/1e	10 cd/m2	3°/s
7	I/1a	4 cd/m2	2°/s

Standard Pseudoisochromatic Plates = SPP), slit-lamp biomicroscopic fundoscopic examination, and blood pressure measurement.

Inclusion criteria of this study consisted of:

Maximum spherical refraction of ±6 diopters (D), maximum cylindrical refraction of ±2 D; distant visual acuity greater than or equal to 1.0 logMAR [20/20] for subjects up to 60 years, greater than or equal to 0.8 logMAR [20/25] for subjects from 61 to 70 years, greater than or equal to 0.63 logMAR [20/30] for subjects older than 70 years; isocoria, pupil diameter greater than 3 mm; IOP (air pulse tonometer) less than or equal to 21 mm Hg; normal anterior segments, ocular fundus: normal appearance of the cup to disc ratio (CDR) less than or equal to 0.5, interocular difference of CDR less than 0.3; and a normal macular region, retinal vessels, and peripheral retinal examination (with undilated pupils).

Exclusion criteria consisted of:

Amblyopia, strabismus, ocular motility disorder, diseases of the retina, glaucoma, glaucoma suspect, macular degeneration, IOP greater than 21 mm Hg, abnormal color vision test (ISPP - Ishihara and Standard Pseudoisochromatic Plates = SPP), history or findings of other neuro-ophthalmological disease, relevant opacities of the central refractive media (cornea, lens, vitreous body), use of miotic drugs, intraocular surgery (except uncomplicated cataract surgery, more than three months previous to testing), keratorefractive surgery (LASIK), drugs influencing reaction time, drugs indicating severe general diseases (antidiabetic pharmaceuticals and antihypertensive medication were allowed for subjects older than 70 years), neurologic conditions, pregnancy, nursing, acute infections, heavy smoking (>10 cigarettes/day), alcohol abuse, diabetic retinopathy, coronary heart disease, stroke, migraine, Raynaud's syndrome, and suspected lack of cooperation and attention,

based on results from the ophthalmologic examination.

Fourteen subjects (two subjects for each of seven age groups, five males and nine females) were examined two more times, at 8-week intervals (0, 8, 16 weeks) to assess test–retest variability. Seven right eyes and seven left eyes were examined for this segment of the investigation.

Examination Procedure

In 2007, Haag Streit AG introduced the Octopus 900 perimeter, which compared with its predecessor, the Octopus 101, is characterized by a smaller cupola radius of 300 mm and higher stimulus luminance values (up to 1260 cd/m^2 or 3970 apostilbs). A major advantage of the Octopus 900 perimeter is that kinetic and static examinations of the entire VF can be performed using the same instrument.

One eye per subject (41 right, 45 left eyes) was included in the study.

Depending on refraction and age, near corrective lenses were provided for testing the central 30° field (isopters I/1e at 3°/s, I/1a at 2°/s). If needed, a brief rest break lasting at most a few minutes, was given between testing the central 30° and peripheral (30°–80°) VF. We used the following seven combinations of Goldmann stimulus sizes, stimulus luminance levels, and angular velocities that are presented in Table 1.

The peripheral five isopters, consisting of 24 vectors (every 15° meridian), were presented in random order, while the innermost isopters (I/1e and I/1a) consisted of 12 vectors (every 30° meridian) as represented in Figure 1. If 6 of any of the 12 stimulus presentations were not seen, testing of this isopter was abandoned. The stimuli moved radially from the periphery toward the center. The start and end points for each vector were predefined to produce shorter examination durations. Vectors with stimulus size V/4e start at the outer border region of the normal VF. Vectors for the examination of isopter III/4e, I/4e, I/3e, I/2e, I/1e, and I/1a originated where the previous isopter finished or, depending on its extent, two-times the SD of the average age-related normal values for the Octopus 101. The stimulus moved along this vector and was controlled electronically. Participants were asked to press the response button as soon as the moving stimulus was perceived. This location was recorded and depicted with an arrowhead for each vector. The program was interrupted if the participant kept the button pressed for longer than several seconds duration. A represen-
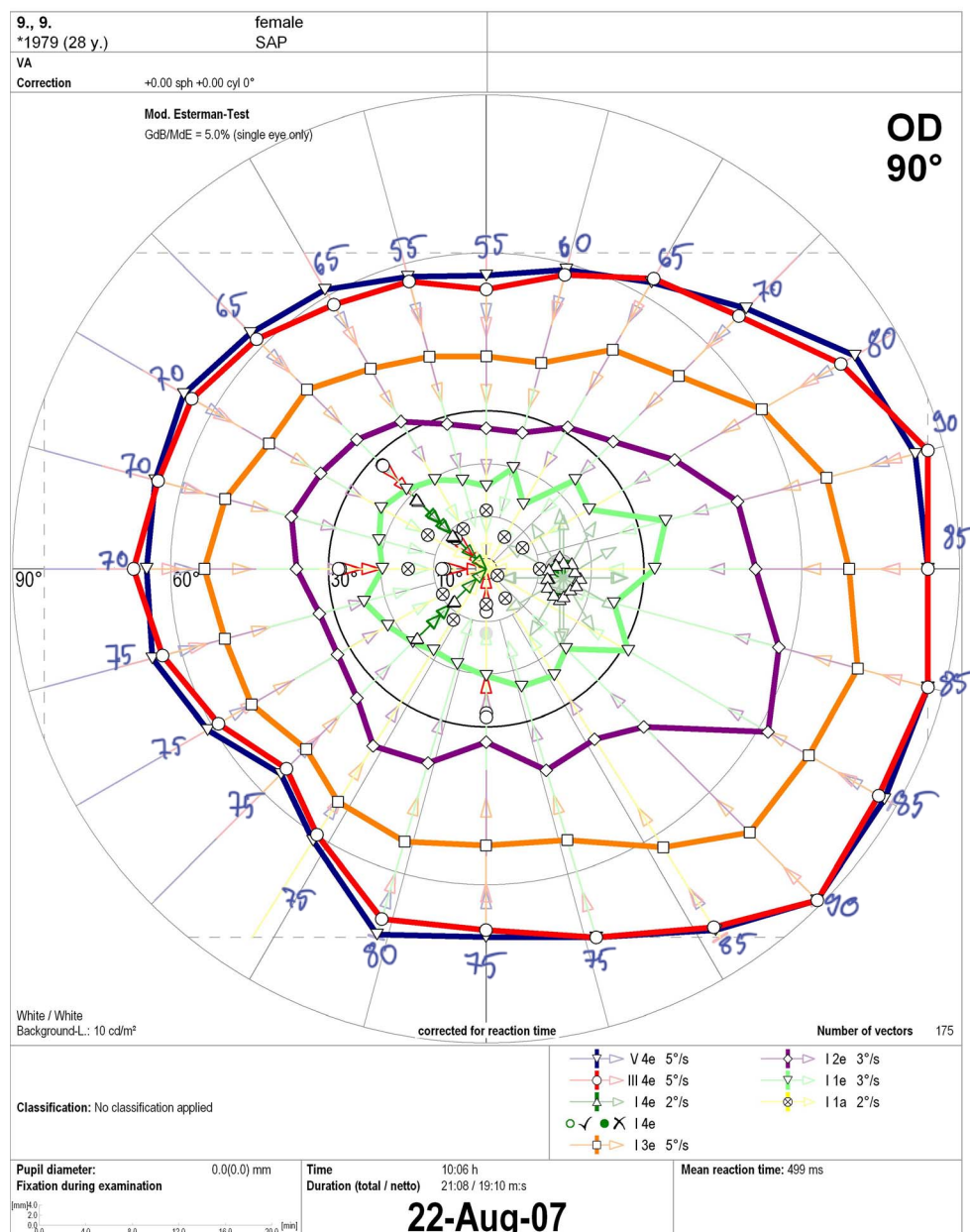
Figure 1. Representative example of a healthy subject with the six examined isopters (the *red double headed arrows* show the RT vectors).

tative example of results obtained for one healthy control subject is presented in Figure 1.

The subjects' response was adjusted according to the individual's RT, which was defined as the time between the start of a static suprathreshold stimulus presentation and the subjects' response. The RT was tested with 12 stimuli using the III/4e target at 5°/s.

These RT vectors were presented twice along the horizontal nasal (0°), oblique (45°), and inferior (270°) meridian at an eccentricity of 10° and 30° (in Fig. 1, the double-head red arrows indicate the RT vectors). If a subject was not attentive, the individual stimulus presentation along the reaction time vectors could be repeated once.

Table 2. The Number, Sex Ratio, Mean Age, SD, Median Age, Per Decade of Age, of the (Analyzed) Participants in Each Cohort (→ One Male, Second Decade of Age was Excluded)

Age group (y)	N subjects	Ratio Male:Female	Mean age ± SD (Range, y)	Median Age, y
I (10–19)	11	5:6	16.8 ± 2.1 (11.7–19.8)	16.7
II (20–29)	13	6:7	25.7 ± 2.2 (20.7–28.8)	25.7
III (30–39)	10	2:8	36.3 ± 2.7 (31.6–39.8)	36.9
IV (40–49)	13	4:9	45.3 ± 3.1 (40.7–49.7)	45.8
V (50–59)	14	6:8	54.9 ± 2.7 (50.7–59.7)	53.8
VI (60–69)	12	4:8	64.8 ± 2.5 (61.7–68.7)	64.8
VII (70–79)	12	6:6	76.0 ± 2.6 (71.7–79.8)	75.8
TOTAL	85	33:52	46.2 ± 19.5 (11.7–79.8)	47.7

Instrument

The background luminance of the cupola of the Octopus 900 perimeter was automatically adjusted to 10 cd/m^2 (9.57–11.49 cd/m^2) or 31.5 apostilbs. The maximum stimulus luminance was 1260 cd/m^2 (3970 apostilbs). The stimuli were presented in random order with a maximum eccentricity of 90° radius in the temporal region of the VF.

Pupil characteristics and eye movements were monitored during the examination by the image produced from an infrared camera inside the cupola. The program discontinued stimulus presentations in the case of eyelid closure or fixation breaks. Fixation monitoring was set to the minimum, meaning that eye movements were allowed to within 3 mm (~2°) from fixation. The examiner corrected the subject's eye and head position manually if necessary.

Analyses

The blind spot area was excluded from the analyses. If the stimulus crossed the vertical midline prior to a response, or if the distance between the beginning and end of a kinetic scan was greater than 30°, the results were excluded. This occurred for nine of the scans for the 1/1a stimulus (2°/s) and for 147 total kinetic scans for all stimuli. These vectors were drawn by hand and were irregular. The results of left eyes were converted into a right eye format for consistency of interpretation.

For the analysis of the kinetic data, we used the JMP software package (version 7.0.1; SAS Institute Inc., Cary, NC) and Program R (A Language and Environment for Statistical Computing; Development Core Team, Foundation for Statistical Computing, Vienna, Austria, 2010, ISBN: 3-900051-07-0, http://www.R-project.org).

Model

We created an age-related and RT-corrected mathematical model, which consisted of a stepwise multiple linear regression mixed-effects model. For the model, the independent variables were age, visual angle (cosine α, sine α), stimulus size, stimulus luminance, stimulus speed (size, luminance, Speed = SLS) and their interactions. Sine (angle), sine (2× angle), cosine (angle), and cosine (2× angle) describe the elliptical shape and sine (angle) × cosine (2× angle) the typical shape of the isopters. In association with the stimulus size and stimulus luminance, these interactions characterize the effects of the facial profile and the temporal extension.[4] A detailed description of the components of the model is included in Appendix A.

Results

Participants/Examination

We examined the full kinetic VF of 86 ophthalmologically healthy subjects (34 males, 52 females, aged between 11 and 79 years, with 10–14 participants per decade of age). Seventy of 86 subjects had already undergone static VF testing in another investigation before being examined in this study. Additionally, 16 healthy individuals, without any perimetric experience, were recruited by friends or relatives of the voluntary participants.

One of the 86 subjects was excluded from the analysis because of an elevated CDR of 0.6. Eighty-five participants (33 males, 52 females) were analyzed, as indicated in Table 2. Isopter I/2e at 3°/s was excluded from the analysis of two subjects (age groups III and VII) because of software difficulties. In one subject (age group VII), because of loss of concen-
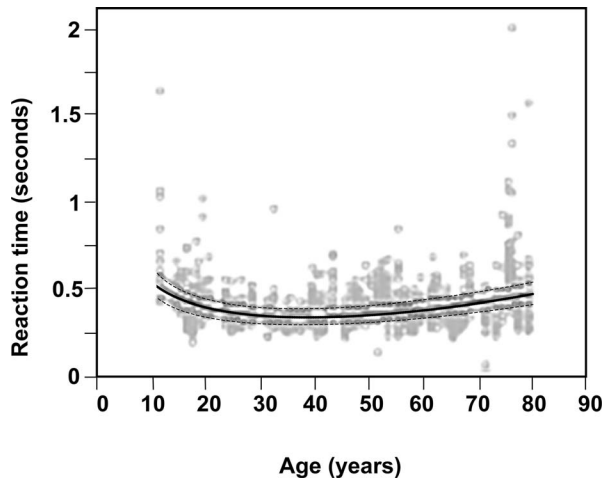
Figure 2. Reaction time (RT) depending on age (the *black line* in the middle shows the predicted RT). Each *gray circle* shows the subjects' RT for the different stimuli. The *dashed lines* present the 95% confidence limits, in which the mean individual RT can be expected.

Figure 3. The graphs demonstrate the extent of the six reaction time-corrected isopters along the nasal meridian as a function of age.

tration and interest, the analysis was restricted to the four peripheral isopters only.

Reaction Time (RT)

We fitted the data to a model that estimated the RT. The mean estimated RT (based on the multiple RT measures obtained at 10° and 30° eccentricity along the nasal, 45° oblique and 270° inferior meridians at 5°/s.) was 393 ms (range, 350–522 ms; median 377 ms). The shortest RT was found in the third age group (30–39), whereas the largest one was in the oldest age (VII, ages 70–79). We observed a decrease of the RT from the first to the third age group, followed by an increase as shown in Figure 2. The median RT at 10° eccentricity was 356 ms and at 30° eccentricity 391 ms. We observed an average increase of the RT of 1.74 ms/°. Subjects' responses were adjusted by the individual RT.

Model

An age-adjusted and RT-corrected mathematical model was created. The fit was satisfactory ($r^2 = 0.94$), indicating that 94% of the measured variance is explained by this model. The adjusted r^2 was identical with this data (because of few parameters used for the model in comparison to the large amount of data). A summary of the model is presented in Appendix A, and details are provided in Appendix B.
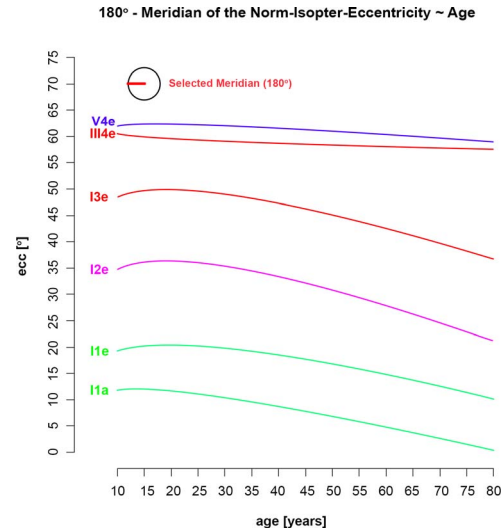
Ageing

The extent of the six RT-corrected isopters for the nasal meridian as a function of age are depicted in Figure 3. For the largest and most intense stimuli (V/4e and III/4e), and the smallest stimulus size and luminance (I/1a) the maximum eccentricity for detection continuously declined with increasing age. For stimulus sizes I/3e, I/2e, and I/1e there was a slight increase in the maximum eccentricity of detection up to the second age group, with a subsequent continuous decline for older ages. The age-related decline was negligible for the largest and most intense stimuli, but was up to approximately 15° for the I/3e and dimmer stimuli. Figure 4 presents the average normal isopter locations for the younger (10–40), middle (40–70), and older (70 and older) age groups.

Test–Retest

The test–retest reliability (three repetitions) of the median absolute value of the eccentricity varied between 5° of eccentricity. No significant learning effect was observed by analyzing the first and second, or first and third examinations for each age group and isopter (Fig. 5).

Discussion

To our knowledge, this is the first study to obtain age-corrected normal kinetic values for the entire VF
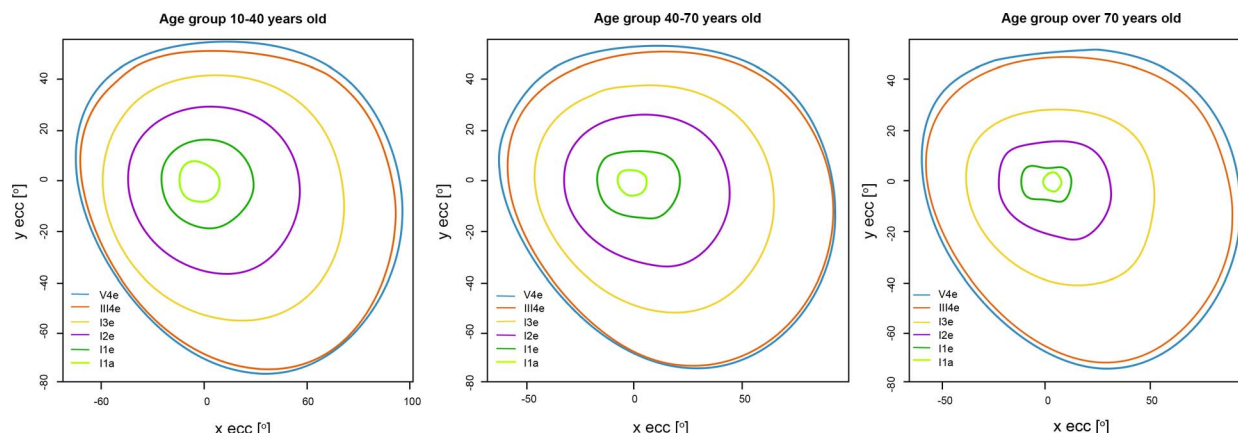
Figure 4. The normal isopters for the three age groups (10- to 40-, 40- to 70- and over 70-years old).

for the new Octopus 900 perimeter, up to an eccentricity of 90°. Age-related normal values are essential for defining and characterizing VF defects. Several investigators have previously published age-related values for kinetic perimetry of various stimulus size and luminance combinations performed manually on the Goldmann perimeter, with some of these publications reporting both the mean and 95% confidence limits for various isopters.[9–12]

Testing the entire VF, especially the peripheral area, is important for the evaluation of complex VF loss.[9] Furthermore, drugs or other therapeutic interventions (such as intravitreal drug delivery systems or systemic medication) may interfere with the entire retina and visual system. For example, in patients receiving an intravitreal anti–vascular endothelial growth factor (VEGF) therapy, these substances

could reduce the neuroprotective effects of VEGF, and thus promote the loss of neural cells in the peripheral retina while preserving function in the central regions. Early glaucomatous VF defects usually occur within the central 30° area, but occasionally VF damage is in the (nasal) peripheral region.[13–15] For neuro-ophthalmologic and retinal disorders, evaluation of the far peripheral VF is also critically important. These are reasons for testing the entire VF, and the peripheral testing takes just 28% of the full VF evaluation.[16] Promising results using a combination of kinetic and static perimetry for subtle peripheral defects were reported by other authors.[17]

We created a mathematical model that describes the age- and RT-corrected normative values for the entire VF as measured by kinetic examination with the new Octopus 900 perimeter. The model fit was
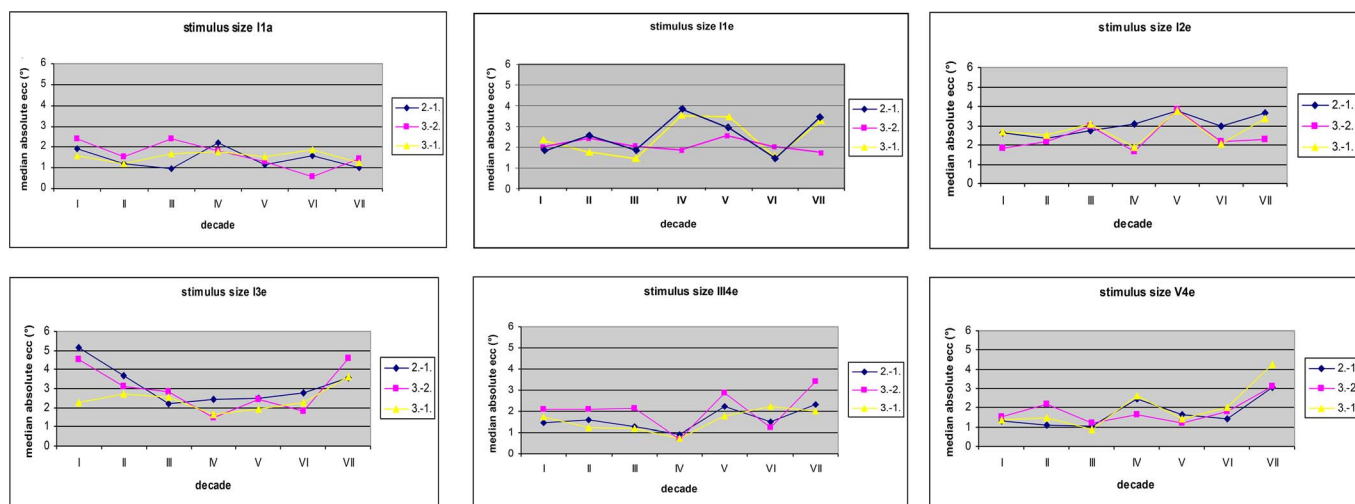

Figure 5. Test–retest analyses for the median of the absolute eccentricity (in degrees) as a function of age per decade for six of the isopters (I/1a, I/13, I/2e, I/3e, III/43, and V/4e). 1 = First Examination, 2 = Second Examination, 3 = Third Examination.

excellent with $r^2 = 0.94$. The adjusted r^2 was in the same range. The local threshold values are of interest for the progression of advanced VF losses and for a screening examination of the peripheral VF in ophthalmologically healthy subjects.[7] Vonthein et al.[4] created a model with a fit of $r^2 = 0.86$, using the Octopus 101 perimeter.

The size of the VF changes with age. A steady decrease occurred with age that was greater in the temporal than in the nasal region. Isopters become closer together with increasing age. This aging process starts in childhood and continues to senescence.[18–20] This is produced by lens density/cataracts,[21,22] reduction of the pupil size, neural losses in the retina and optic nerve,[23] a greater loss of scotopic than photopic sensitivity through adulthood,[24] a decrease of photo-receptors,[25] displacement of nuclei,[26] and other ana-tomical changes with aging.[19] A reduction of the axonal diameter and a redistribution of the fiber diameter of the optic nerve has also been observed.[27–29] An accelerated loss of the differential luminance sensitivity and spatial resolution was found in older subjects.[30–32] A greater influence of the stimulus velocity with increasing age for the central isopters has been reported.[33] For smaller and dimmer stimuli only, an age-dependence was observed.[4] Paetzold et al. (personal communication, 2004) found a decrease for those stimuli of 1° per decade. Without knowledge of the stimulus size, we observed a median decrease for all age groups of 0.8° eccentricity per decade. We expected a diminution of the median eccentricity with age for all age groups. This aging effect was seen for light and bright stimuli as well as smaller and dimmer targets (III/4e, I/3e, I/2e, and I/1e). The ceiling effect of the greatest stimuli is also mentioned here, firstly because of the technical limits of the Octopus perimeter and secondly there is currently no larger or brighter stimulus size than V4e.

The measurement of the RT is of special interest in subjects with retinal or neurological diseases and in older participants.[2,33] The individual RT corrected response can minimize the systemic, subject-related measurement errors of the local kinetic thresholds (Wabbels BK, et al. IOVS. 2001;42: ARVO Abstract S852). Without measuring the RT, it can be difficult to decide whether a VF loss is the result of true damage or from an increased RT.[4] The RT increases with eccentricity and with age,[20] and decreases with higher stimulus luminances (Paetzold et al., personal communication, 2004). We observed an increase of the RT of 1.74ms/°, which is in the same range as observed by other authors[35–38] for the 30° or 50°

eccentricity VF. The RT was shortest in the fovea and became greater with increasing eccentricity; a shorter RT was observed in the nasal than the temporal field.[36,37] By accounting for individual differences in RT, this technique provides a greater level of standardized testing for clinical centers. Additionally, RT has been found to be a significant factor in VF determinations.[39,40]

Schiefer et al.[2] found the local variability to be greatest temporally with eccentricity, greatest inferior-nasally related to the anatomical region of the nose, and smallest inferior-temporally overall. The instru-ment used and the anatomy had a greater effect on the peripheral isopters with a large and bright stimulus.[4] Parrish et al.[41] observed a greater variability in the peripheral area, especially temporal, because of a flatter slope of the VF profile of sensitivity in this region.

Knowledge of the normal test–retest reliability is essential for the interpretation of the results of kinetic perimetry. All examinations and retest data are based on many factors, including time of day, training, fatigue, attention, room temperature, and the techni-cian.[29,39] Learning effects[42] were found to be more pronounced in the peripheral VF than in the paracentral regions.[39] Although Drance et al.[19] found no significant learning effect in his series, others have concluded that learning effects occur and may interfere with correct interpretation of series of follow-up VFs.[42] Test–retest reliability overall was less than 1.2° was measured by Schiefer et al.[10]

Conclusion

A mathematical model is introduced that allows a prediction of local kinetic threshold for the different isopters, based on age-related and RT-corrected normative data for the entire 90° VF, using the new Octopus 900 perimeter. This mathematical model serves as a foundation for establishing age-related properties of the entire VF for automated kinetic perimetry, and provides a basis for quantitative analysis and interpretation of VFs in a manner similar to that available for automated static perimetry.

Acknowledgments

References

1. Schiefer U, Pätzold J, Dannheim F. Conventional techniques of visual field examination Part 2: confrontation visual field testing–kinetic perimetry [in German]. *Ophthalmologe*. 2005;102:821–827.

2. Schiefer U, Rauscher S, Hermann A et al. Realization of semi-automated kinetic perimetry (SKP) with Interzeag 101 instrument. In: Wall M, Mills RP. eds. *Perimetry Update 2002/2003*. The Hague, the Netherlands: Kugler Publications; 2003:233–238.

3. Niederhauser S, Mojon DS. Normal isopter position in the peripheral visual field in Goldmann kinetic perimetry. *Ophthalmologica*. 2002; 216:406–408.

4. Vonthein R, Rauscher S, Paetzold J et al. The normal age-corrected and reaction time-corrected isopter derived by semi-automated kinetic perimetry. *Ophthalmology*. 2007;114:1065–1072.

5. Schiefer U, Schiller J, Paetzold J et al. Evaluation ausgedehnter Gesichtsfelddefekte mittels computerassistierter kinetischer Perimetrie. *Klin Monatsbl Augenheilkd*. 2001;218:13–20.

6. Schiefer U, Nowomiejska KE, Pätzold J. Semi-automated kinetic perimetry for assessment of advanced glaucomatous visual field loss. In: Grehn F, Stamper R, eds. *Glaucoma*. Berlin, Germany: Springer; 2004:51–61.

7. Wabbels BK, Kolling G. Automatische kinetische Perimetrie mit unterschiedlichen Prüfgeschwindigkeiten. *Ophthalmologe*. 2001; 98:168–173.

8. Keltner JL, Johnson CA, Spurr JO, Beck RW; for the Optic Neuritis Study Group. Comparison of central and peripheral visual field properties in the Optic Neuritis Treatment Trial (ONTT). *Am J Ophthalmol*. 1999, 128:543–553.

9. Goldmann H. Ein selbstregistrierendes Projektionskugelperimeter. *Ophthalmologica*. 1945;109: 71–79.

10. Egge K. The visual field in normal subjects. *Acta Ophthalmologica Supplement*. 1984;169:1–64.

11. Niederhauser S, Mojon DS. Normal isopter position in the peripheral visual field in Goldmann kinetic perimetry. *Ophthalmologica*. 2002; 216:406–408.

12. Anderson DR. Perimetry With and Without Automated. 2nd ed. St Louis: Cv Mosby Auflage; 1987.

13. Schiefer U, Schiller J, Dietrich TJ et al. Evaluation of advanced visual field loss with computer-assisted kinetic perimetry. In: Wall M, Mills RP, eds. *Perimetry Update 2000/2001*. The Hague, the Netherlands: Kugler Publications; 2001:131–136.

14. Werner EB, Beraskow J. Peripheral nasal field defects in glaucoma. *Ophthalmology*. 1979;86: 1875–1878.

15. Caprioli J, Spaeth GL. Static threshold examination of the peripheral nasal visual field in glaucoma. *Arch Ophthalmol*. 1985;103:1150–1154.

16. Stewart WC. Static versus kinetic testing in the nasal peripheral field in patients with glaucoma. *Acta Ophthalmol Copenh*. 1992;70:79–84.

17. Stewart WC, Shields MB, Ollie AR. Peripheral visual field testing by automated kinetic perimetry in glaucoma. *Arch Ophthalmol*. 1988;106:202–206.

18. Pineles SL, Volpe NJ, Miller-Ellis E, et al. Automated combined kinetic and static perimetry: an alternative to standard perimetry in patients with neuro-ophthalmic disease and glaucoma. *Arch Ophthalmol*. 2006;124:363–369.

19. Haas A, Flammer J, Schneider U. Influence of age on the visual fields of normal subjects. *Am J Ophthalmol*. 1986;101:199–203.

20. Drance SM, Berry V, Hughes A. Studies on the effects of age on the central and peripheral isopters of the visual field in normal subjects. *Am J Ophthalmol*. 1967;63:1667–1672.

21. Egge K. The visual field in normal subjects. *Acta Ophthalmol Suppl*. 1984;169:1–64.

22. Costagliola C, Iuliano G, Rinaldi E et al. In vivo measurement of human lens aging using the lens opacity meter. *Ophthalmologica*. 1989;199:158–161.

23. de Natale R, Flammer J, Zulauf M, Bebie T. Influence of age on the transparency of the lens in normals: a population study with help of the Lens Opacity Meter 701. *Ophthalmologica*. 1988;197: 14–18.

24. Johnson CA, Adams AJ, Lewis RA. Evidence for a neural basis of age-related visual field loss in normal observers. *Invest Ophthalmol Vis Sci*. 1989;30:2056–2064.

25. Curcio CA. Photoreceptor topography in ageing and age-related maculopathy. *Eye (Lond)*. 2001; 15:376–383.

26. Gao H, Hollyfield JG. Aging of the human retina. Differential loss of neurons and retinal

pigment epithelial cells. *Invest Ophthalmol Vis Sci*. 1992;33:1–17.

27. Gartner S, Henkind P. Aging and degeneration of the human macula. 1. Outer nuclear layer and photoreceptors. *Br J Ophthalmol*. 1981;65:23–28.

28. Repka MX, Quigley HA. The effect of age on normal human optic nerve fiber number and diameter. *Ophthalmology*. 1989;96:26–32.

29. Devaney KO, Johnson HA. Neuron loss in the aging visual cortex of man. *J Gerontol*. 1980;35:836–841.

30. Balazsi AG, Rootman J, Drance SM, Schulzer M, Douglas GR. The effect of age on the nerve fiber population of the human optic nerve. *Am J Ophthalmol*. 1984;97:760–766.

31. Lachenmayr BJ, Kojetinsky S, Vivell PMO. Is there an accelerated loss at older age for normal sensitivity in the central visual field? In: Wall M, Mills RP, eds. *Perimetry Update 1994/1995*. The Hague, the Netherlands: Kugler Publications; 1995:49–56.

32. Wall M, Chauhan BC, Frisén L, House PH, Brito C. Visual field of high-pass resolution perimetry in normal subjects. *J Glaucoma*. 2004;13:15–21.

33. Iwase A, Kitazawa Y, Ohno Y. On age-related norms of the visual field. *Jpn J Ophthalmol*. 1988;32:429–437.

34. Fankhauser F. Kinetische Perimetrie. *Ophthalmologica*. 1969;158:406–418.

35. Rauscher S, Sadowski B, Vonthein R et al. Assessment of reaction times in order to enhance quality of semi-automated kinetic perimetry (SKP) - an age-related normative study. In: Wall M, Mills RP, eds. *Perimetry Update 2002/2003*. The Hague, the Netherlands: Kugler Publications; 2003:353–358.

36. Schiefer U, Strasburger H, Becker ST et al. Reaction time in automated kinetic perimetry: effects of stimulus luminance, eccentricity, and movement direction. *Vision Res*. 2001;41:2157–2164.

37. Wall M, Kutzko KE, Chauhan BC. The relationship of visual threshold and reaction time to visual field eccentricity with conventional automated perimetry. *Vision Res*. 2002;42:781–787.

38. Osaka N. Naso-temporal differences in human reaction time in the peripheral visual field. *Neuropsychologia*. 1978;16:299–303.

39. Becker ST, Vonthein R, Volpe NJ, Schiefer U. Factors influencing reaction time during automated kinetic perimetry on the Tuebingen Computer Campimeter. *Invest Ophthalmol Vis Sci*. 2005;46:2633–2638.

40. Henson DB, Artes PH. New developments in supra-threshold perimetry. *Ophthalmic Physiol Opt*. 2002;22:463–468.

41. Artes PH, McLeod D, Henson DB. Response time as a discriminator between true- and false-positive responses in suprathreshold perimetry. *Invest Ophthalmol Vis Sci*. 2002;43:129–132.

42. Parrish RK, Schiffman J, Anderson DR. Static and kinetic visual field testing - reproducibility in normal volunteers. *Arch Ophthalmol*. 1984;102:1497–1502.

43. Heijl A, Lindgren G, Olsson J. The effect of perimetric experience in normal subjects. *Arch Ophthalmol*. 1989;107:81–86.

Appendix A: A Summary of the Full Results of the Mathematical Model for Automated Kinetic Perimetry

Intercept: 34.1081779

Age:

Age	ln (age)
−0.2572225	4.50957638

Stimulus condition:

I/2e at 3°/s	I/1e at 3°/s	I/1a at 2°/s	I/3e at 5°/s	III/4e at 5°/s	V/4e at 5°/s
−22.390857	−28.717235	−22.595572	0.85379893	31.4617962	0

Shape

Sine (Angle)	Cosine (Angle)	Sine (2 × Angle)	Cosine (2 × Angle)	Sine (Angle) × Cosine (2 × Angle)
−4.0582332	7.65641149	−3.1203881	5.25169817	0.71985225

Two Way Interactions

Age × Stimulus condition:

	I/2e at 3°/s	I/1e at 3°/s	I/1a at 2°/s	I/3e at 5°/s	III/4e at 5°/s	V/4e at 5°/s
Age	−0.3074818	−0.1062584	0.18978096	−0.2098779	0.17008673	0
ln (age)	7.80908545	2.62608475	−5.2591494	4.61051333	−3.2546707	0

Shape × Stimulus condition:

	I/2e at 3°/s	I/1e at 3°/s	I/1a at 2°/s	I/3e at 5°/s	III/4e at 5°/s	V/4e at 5°/s
Sine (Angle)	0.91357785	2.94593071	3.6172081	−1.6889509	−3.6931811	0
Cosine (Angle)	−10.349968	−7.432776	−1.1932089	−1.880416	3.12988685	0
Sine (2 × Angle)	1.24542429	2.56052065	2.93460231	0.01257351	−3.396913	0
Cosine (2 × Angle)	−0.7696372	−2.3631974	−4.1091768	0.77283898	3.25164945	0
Sine (Angle) × Cosine (2 × Angle)	−0.6587454	−0.1317541	−0.1947873	−0.7457717	0.22478461	0

Three Way Interaction

Age × Shape × Stimulus condition

	I/2e at 3°/s	I/1e at 3°/s	I/1a at 2°/s	I/3e at 5°/s	III/4e at 5°/s	V/4e at 5°/s
Age × cosine (angle)	−0.107209	−0.0476162	0.20596294	−0.0771797	−0.0769468	0
ln (age) × cosine (angle)	3.41882728	0.86278211	−4.4344809	1.65190687	2.38335733	0

SD: 6.01281607

Appendix B: The Full Results of the Mathematical Model for Automated Kinetic Perimetry

Term	Estimate
Intercept	34.1081779
Size/intensity/speed [1 10 3]	−22.390857
Size/intensity/speed [1 15 3]	−28.717235
Size/intensity/speed [1 19 2]	−22.595572
Size/intensity/speed [1 5 5]	0.85379893
Size/intensity/speed [3 0 5]	31.4617962
Sine (angle)	−4.0582332
Cosine (angle)	7.65641149
Sine (2 × angle)	−3.1203881
Cosine (2 × angle)	5.25169817
Sine (angle) cosine (2 × angle)	0.71985225
Size/intensity/speed [1 10 3] × sine (angle)	0.91357785
Size/intensity/speed [1 15 3] × sine (angle)	2.94593071
Size/intensity/speed [1 19 2] × sine (angle)	3.6172081
Size/intensity/speed [1 5 5] × sine (angle)	−1.6889509
Size/intensity/speed [3 0 5] × sine (angle)	−3.6931811
Size/intensity/speed [1 10 3] × cosine (angle)	−10.349968
Size/intensity/speed [1 15 3] × cosine (angle)	−7.432776
Size/intensity/speed [1 19 2] × cosine (angle)	−1.1932089
Size/intensity/speed [1 5 5] × cosine (angle)	−1.880416
Size/intensity/speed [3 0 5] × cosine (angle)	3.12988685
Size/intensity/speed [1 10 3] × sine (2 × angle)	1.24542429
Size/intensity/speed [1 15 3] × sine (2 × angle)	2.56052065
Size/intensity/speed [1 19 2] × sine (2 × angle)	2.93460231
Size/intensity/speed [1 5 5] × sine (2 × angle)	0.01257351
Size/intensity/speed [3 0 5] × sine (2 × angle)	−3.396913
Size/intensity/speed [1 10 3] × cosine (2 × angle)	−0.7696372
Size/intensity/speed [1 15 3] × cosine (2 × angle)	−2.3631974
Size/intensity/speed [1 19 2] × cosine (2 × angle)	−4.1091768
Size/intensity/speed [1 5 5] × cosine (2 × angle)	0.77283898
Size/intensity/speed [3 0 5] × cosine (2 × angle)	3.25164945
Size/intensity/speed [1 10 3] × sine (angle) × cosine (2 × angle)	−0.6587454
Size/intensity/speed [1 15 3] × sine (angle) cosine (2 × angle)	−0.1317541
Size/intensity/speed [1 19 2] × sine (angle) × cosine (2 × angle)	−0.1947873
Size/intensity/speed [1 5 5] × sine (angle) × cosine (2 × angle)	−0.7457717
Size/intensity/speed [3 0 5]] × sine (angle) × cosine (2 × angle)	0.22478461
Age	−0.2572225
ln age	4.50957638
Age × size/intensity/speed [1 10 3]	−0.3074818
Age × size/intensity/speed [1 15 3]	−0.1062584
Age × size/intensity/speed [1 19 2]	0.18978096
Age × size/intensity/speed [1 5 5]	−0.2098779

Continued.

Term	Estimate
Age × size/intensity/speed [3 0 5]	0.17008673
ln age × size/intensity/speed [1 10 3]	7.80908545
ln age × size/intensity/speed [1 15 3]	2.62608475
ln age × size/intensity/speed [1 19 2]	−5.2591494
ln age × size/intensity/speed [1 5 5]	4.61051333
ln age × size/intensity/speed [3 0 5]	−3.2546707
Age × size/intensity/speed [1 10 3] × cosine (angle)	−0.107209
Age × size/intensity/speed [1 15 3] × cosine (angle)	−0.0476162
Age × size/intensity/speed [1 19 2] × cosine (angle)	0.20596294
Age × size/intensity/speed [1 5 5] × cosine (angle)	−0.0771797
Age × size/intensity/speed [3 0 5] × cosine (angle)	−0.0769468
ln age × size/intensity/speed [1 10 3] × cosine (angle)	3.41882728
ln age × size/intensity/speed [1 15 3] × cosine (angle)	0.86278211
ln age × size/intensity/speed [1 19 2] × cosine (angle)	−4.4344809
ln age × size/intensity/speed [1 5 5] × cosine (angle)	1.65190687
ln age × size/intensity/speed [3 0 5] × cosine (angle)	2.38335733
Sigma	6.01281607